

Electromechanical characterization of $\text{Pb}(\text{In}_{0.5}\text{Nb}_{0.5})\text{O}_3\text{-Pb}(\text{Mg}_{1/3}\text{Nb}_{2/3})\text{O}_3\text{-PbTiO}_3$ crystals as a function of crystallographic orientation and temperature

Shujun Zhang,^{1,a)} Jun Luo,² Wesley Hackenberger,² Nevin P. Sherlock,³ Richard J. Meyer, Jr.,³ and Thomas R. Shrout¹

¹Materials Research Institute, Pennsylvania State University, University Park, Pennsylvania 16802, USA

²TRS Technologies, Inc., 2820 East College Avenue, State College, Pennsylvania 16801, USA

³Applied Research Laboratory, Pennsylvania State University, University Park, Pennsylvania 16802, USA

(Received 24 February 2009; accepted 11 April 2009; published online 22 May 2009)

Relaxor based $\text{Pb}(\text{In}_{0.5}\text{Nb}_{0.5})\text{O}_3\text{-Pb}(\text{Mg}_{1/3}\text{Nb}_{2/3})\text{O}_3\text{-PbTiO}_3$ ternary single crystals (PIN-PMN-PT) were reported to have broader temperature usage range (T_{R-T}) and comparable piezoelectric properties to $\text{Pb}(\text{Mg}_{1/3}\text{Nb}_{2/3})\text{O}_3\text{-PbTiO}_3$ (PMNT) crystals. In this work, the orientation dependent dielectric, piezoelectric and electromechanical properties for PIN-PMN-PT crystals were investigated along $\langle 001 \rangle$ and $\langle 110 \rangle$ directions. The electromechanical couplings k_{33} and k_{32} for $\langle 110 \rangle$ poled crystals were found to be 0.91 and 0.91, respectively, with piezoelectric coefficients d_{33} and d_{32} on the order of 925 and -1420 pC/N. Of particular significance was the mechanical quality factor Q_{33} for $\langle 110 \rangle$ oriented crystals, which was found to be ≥ 500 , much higher than the Q values of $\langle 001 \rangle$ oriented relaxor-PT crystals ($Q \sim 70\text{--}200$). The temperature dependence of the piezoelectric properties exhibited good temperature stability up to their ferroelectric phase transition $T_{R-T} \sim 125$ °C, indicating $\langle 001 \rangle$ and $\langle 110 \rangle$ oriented PIN-PMN-PT are promising materials for transducer applications, with the latter for high power resonant devices where low loss (high Q) was required. © 2009 American Institute of Physics. [DOI: 10.1063/1.3131622]

I. INTRODUCTION

Recently, extensive research has been carried out on relaxor-PT ferroelectric single crystals. As reported, domain engineered $\text{Pb}(\text{Zn}_{1/3}\text{Nb}_{2/3})\text{O}_3\text{-PbTiO}_3$ (PZNT) and $\text{Pb}(\text{Mg}_{1/3}\text{Nb}_{2/3})\text{O}_3\text{-PbTiO}_3$ (PMNT) crystals oriented along the pseudocubic $\langle 001 \rangle$ direction exhibit high electromechanical coupling factors and piezoelectric coefficients for longitudinal mode. Electromechanical coupling factors on the order of >0.90 and piezoelectric coefficients higher than 1200 pC/N are common for all relaxor-PT single crystals.¹⁻⁴ The transverse piezoelectric response for relaxor-PT perovskite crystals is more complicated, where it has been reported that there are four different vibration modes showing good piezoelectric characteristics. These modes are $(001)/\langle 100 \rangle$, $(001)/\langle 110 \rangle$, $(110)/\langle 001 \rangle$, and $(110)/\langle -110 \rangle$, where the first number indicates the electrode face and the second number is the acoustic wave propagation direction.⁵ It has been demonstrated that the highest transverse piezoelectric coefficients are obtained from crystals poled along $\langle 110 \rangle$ and vibrated along the $\langle 001 \rangle$ direction,⁵⁻¹⁰ with small signal d_{32} coefficients on the order of ~ -1500 pC/N and electromechanical coupling factor $k_{32} \sim 0.90$ in PZNT and PMNT crystals.

Regardless of the excellent piezoelectric properties found in PZNT and PMNT ferroelectric crystals, the crystals exhibit relatively low Curie and ferroelectric phase transition temperatures ($T_{R-T} \sim 60\text{--}95$ °C), limiting the operating temperature range. Thus, numerous studies are focusing on ex-

ploring new high performance ferroelectric crystals with higher Curie and ferroelectric phase transition temperatures. Based on the reported data in polycrystalline relaxor-PT systems, crystal growth has been carried out on the $\text{Pb}(\text{Sc}_{0.5}\text{Nb}_{0.5})\text{O}_3\text{-PbTiO}_3$, $\text{Pb}(\text{In}_{0.5}\text{Nb}_{0.5})\text{O}_3\text{-PbTiO}_3$, $\text{Pb}(\text{Yb}_{0.5}\text{Nb}_{0.5})\text{O}_3\text{-PbTiO}_3$, and $\text{BiScO}_3\text{-PbTiO}_3$ systems, using high temperature solution and/or flux Bridgman methods.¹¹⁻²¹ Though the crystals obtained were confirmed to exhibit high T_{CS} and T_{R-T} s, their implementations were restricted by the crystal size and/or crystal quality. More recently, solid state crystal growth of PMN-PZ-PT²²⁻²⁴ and melt Bridgman growth of PIN-PMN-PT²⁵⁻²⁷ ternary single crystals have been reported, showing broadened temperature usage range $T_{R-T} > 100$ °C. These crystals can be grown to large size and of high quality. In addition to the efforts to improve T_{R-T} , higher mechanical Q values in the relaxor-PT ferroelectric crystals have been observed in recent studies. The Q was found to be a function of composition and crystallographic directions, while maintaining electromechanical coupling on the order of 0.90.²⁸

In this work, ternary PIN-PMN-PT single crystals with high T_{R-T} (>125 °C) were selected for further investigation along different crystallographic orientations $\langle 001 \rangle$ and $\langle 110 \rangle$ for longitudinal/transverse modes. The temperature dependence of the dielectric, piezoelectric, and electromechanical behaviors were explored for use at elevated temperature.

II. EXPERIMENTAL

Ternary $x\text{PIN}-(1-x-y)\text{PMN}-y\text{PT}$ ($x > 0.2 \sim 0.4$; $y > 0.28 \sim 0.33$) rhombohedral single crystals grown by Bridg-

^{a)}Author to whom correspondence should be addressed. Electronic mail: soz1@psu.edu.

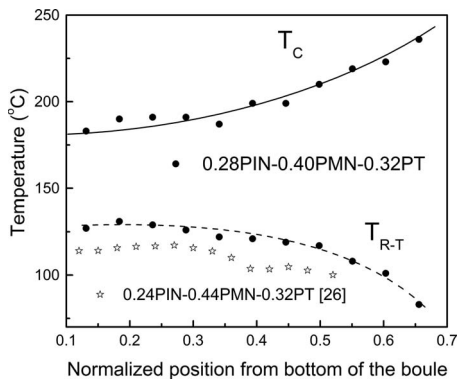


FIG. 1. Curie temperature and ferroelectric phase transition temperature along the growth direction for 0.28PIN–0.40PMN–0.32PT single crystal.

man method were investigated in detail. These crystals demonstrated improved temperature stability and broadened operating temperature range.²⁷ Due to the different segregation ratio of the ions in crystal, the grown single crystal boules exhibited compositional variation along the growth direction. The composition along the growth direction was determined by electronic probe microanalysis, the PIN variation was found to be less than 2% from the bottom to the top of the crystal boule (100mm in length and 50mm in diameter). In contrast, the variations are found to be on the order of 5% and 7% for PMN and PT, respectively. Figure 1 shows Curie temperatures (T_C) and rhombohedral to tetragonal phase transition (T_{R-T}) temperatures for $\langle 001 \rangle$ poled crystals, cut from different positions along the growth direction of a nominal 0.28PIN–0.40PMN–0.32PT crystal. 20%–30% of the crystal boule belongs to the tetragonal phase due to the high PT content. It was found that the Curie temperature ranged from 175 to 230 °C, while T_{R-T} fell in the range of 138–90 °C along the growth direction. Compared to 0.24PIN–0.44PMN–0.32PT crystal from Ref. 26, the T_{R-T} was found to be increased by 15–20 °C. It was observed that one third of the grown 0.28PIN–0.40PMN–0.32PT crystals possessed T_{R-T} in the range of 120–130 °C and exhibited high piezoelectric properties.

In this work, the 0.28PIN–0.40PMN–0.32PT crystals were grown using the modified Bridgman technique. The crystals were oriented using real-time Laue X-ray and cut to obtain longitudinal rods and transverse bars with the aspect ratios following IEEE piezoelectric standards.^{21,29} All the samples were oriented along $\langle 001 \rangle$ and $\langle 110 \rangle$ directions and vacuum sputtered gold was applied as the electrodes. For the transverse mode, configurations used in this study were bars with electrodes on (001) or (110) faces and length (vibration) along $\langle 100 \rangle / \langle 110 \rangle$ and $\langle 001 \rangle / \langle -110 \rangle$ directions. All samples were poled by applying 10 kV/cm dc electric field at a temperature of 140 °C. High field polarization and strain measurements were performed on the $\langle 001 \rangle$ and $\langle 110 \rangle$ oriented plate samples at room temperature at a frequency of 1Hz, using a modified Sawyer–Tower circuit and linear variable differential transducer driven by a lock-in amplifier. Room temperature dielectric, piezoelectric, electromechanical properties, and the mechanical loss (inverse of Q) were determined for longitudinal and transverse modes according to

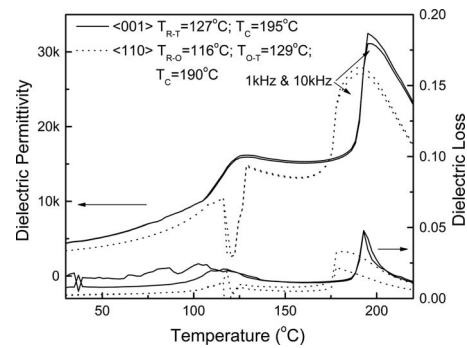


FIG. 2. Dielectric permittivity and dielectric loss as a function of temperature for $\langle 001 \rangle$ and $\langle 110 \rangle$ poled PIN-PMN-PT single crystals, measured at 1 and 10 kHz frequencies.

IEEE standards, by using HP4194A Impedance-phase gain analyzer. The dielectric temperature dependence was measured using a multifrequency LCR meter (HP4284A), connected to a computer controlled temperature chamber. The high temperature piezoelectric and electromechanical characteristics were obtained from an impedance analyzer connected to a temperature chamber. In order to minimize the stress effects on the samples during the measurement, thin silver wires were attached on the electrodes using a small amount of high temperature conductive silver.

III. RESULTS AND DISCUSSION

A. Dielectric properties

Figure 2 shows the dielectric behavior as a function of temperature for $\langle 001 \rangle$ and $\langle 110 \rangle$ poled PIN-PMN-PT single crystals, measured at frequencies of 1 and 10 kHz, respectively. The Curie temperature T_C and ferroelectric phase transition temperatures can be determined by the temperature where the dielectric permittivity reaching its peak values. Thus, the T_C and rhombohedral to tetragonal phase transition temperature T_{R-T} were found to be on the order of 195 and 127 °C for $\langle 001 \rangle$ poled samples, respectively. In contrast, two ferroelectric phase transformations were observed below its Curie temperature for $\langle 110 \rangle$ poled sample. A relatively low dielectric permittivity (~ 2700) in the temperature range of 116 and 129 °C was found, which is believed to be related to an orthorhombic phase, bounded by a lower temperature domain engineered pseudorhombohedral phase and higher temperature tetragonal phase.^{10,30} Thus, the two ferroelectric phase transformation temperatures can be confirmed to be rhombohedral to orthorhombic phase transition $T_{R-O} \sim 116$ °C and orthorhombic to tetragonal phase transition $T_{O-T} \sim 129$ °C, while the Curie temperature was similar to $\langle 001 \rangle$ poled samples.

B. High field ferroelectric properties

Figure 3 shows polarization hysteresis and butterfly strain loops for $\langle 001 \rangle$ [Fig. 3(a)] and $\langle 110 \rangle$ oriented [Fig. 3(b)] PIN-PMN-PT single crystals, respectively. It was found that the coercive field E_C , on the same order of ~ 5 kV/cm for both orientations, much higher than the binary PMNT counterpart (~ 2.5 kV/cm). However, the spontaneous and

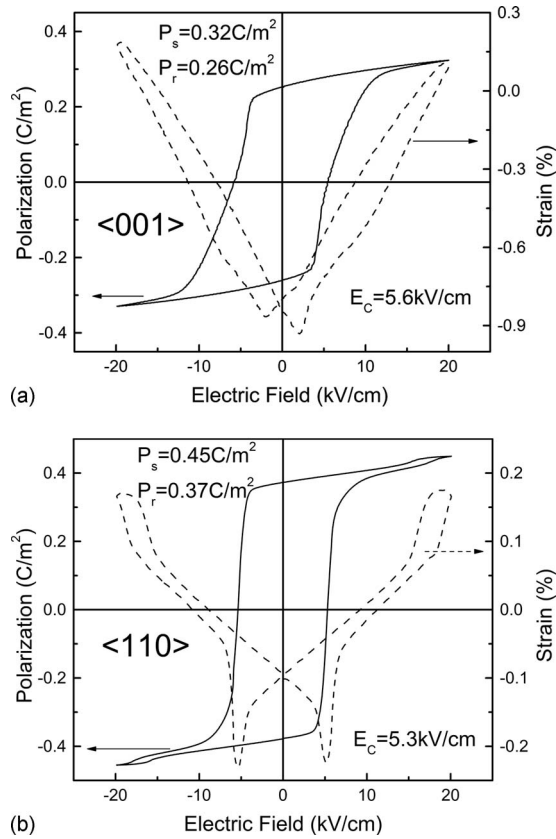


FIG. 3. Bipolar polarization hysteresis and strain butterfly loops for $\langle 001 \rangle$ (a) and $\langle 110 \rangle$ (b) oriented PIN-PMN-PT single crystals.

remnant polarizations exhibited anisotropic behavior, with remnant polarization P_r on the order of 0.26 C/m^2 for $\langle 001 \rangle$ orientation, much lower than the value of the $\langle 110 \rangle$ orientation ($P_r = 0.37 \text{ C/m}^2$). In rhombohedral ferroelectric single crystals, the spontaneous polarization is along the crystallographic $\langle 111 \rangle$ direction. For the domain engineered single crystals along $\langle 001 \rangle$ and $\langle 110 \rangle$ directions, the P_r will be lower than the value along the polar axis $\langle 111 \rangle$, following $P_{r\langle 001 \rangle} \sim 1/\sqrt{2}P_{r\langle 110 \rangle} \sim 1/\sqrt{3}P_{r\langle 111 \rangle}$.^{1,8} As expected, the ratio of the obtained P_r along $\langle 001 \rangle$ and $\langle 110 \rangle$ directions was indeed very close to the theoretical value. The unipolar strain behavior as a function of electric field for the $\langle 001 \rangle$ and $\langle 110 \rangle$ directions are given in Fig. 4. The slope of the strain electric field curve for the $\langle 110 \rangle$ orientation was found to be $\sim 950 \text{ pm/V}$, lower than the value of $\langle 001 \rangle$ orientation $\sim 1520 \text{ pm/V}$, both values are similar to the piezoelectric d_{33} obtained according to IEEE standards (as listed in Table I). The electric field induced phase transformation for $\langle 001 \rangle$ orientation was found to occur at an electric field of $\sim 46 \text{ kV/cm}$ (as shown in the small inset of Fig. 4), while the rhombohedral to orthorhombic phase transformation occurred at a field of $\sim 16 \text{ kV/cm}$ for $\langle 110 \rangle$ orientation, much lower than the threshold for $\langle 001 \rangle$ oriented crystals. The lower threshold electric field indicates the polarization rotation is much easier to be induced through an intermediate phase M_B (“structure bridge” which is anhysteretic in character) when the field applied along $\langle 110 \rangle$ direction, as observed in PMNT crystals.^{30,31}

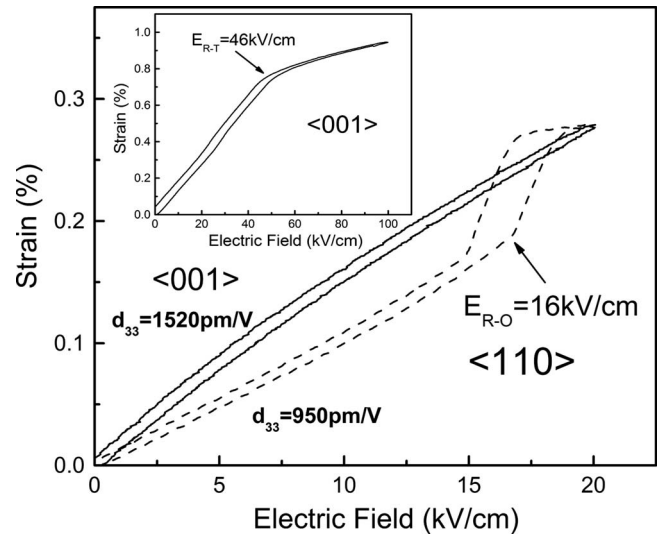


FIG. 4. Unipolar strain behavior as a function of electric field for $\langle 001 \rangle$ and $\langle 110 \rangle$ oriented crystals, showing the electric field induced phase transformation.

C. Room temperature piezoelectric properties of the PIN-PMN-PT crystals

The main properties for longitudinal and transverse modes at room temperature are listed in Table I. The dielectric permittivity was found to be on the order of 4400 and 3400 for $\langle 001 \rangle$ and $\langle 110 \rangle$ poled PIN-PMN-PT crystals, respectively, while the dielectric losses were 0.4% and 0.2%, respectively. The longitudinal electromechanical coupling factor k_{33} was found to be 0.92 for $\langle 001 \rangle$ samples, slightly higher than that of $\langle 110 \rangle$ poled crystals (~ 0.91). The piezoelectric d_{33} was on the order of 1500 pC/N for the $\langle 001 \rangle$ cut, higher than the value for $\langle 110 \rangle$ oriented sample $\sim 925 \text{ pC/N}$. Of particular significance was the mechanical quality factor Q , being greater than 500 for $\langle 110 \rangle$ poled crystals, much higher than the values along $\langle 001 \rangle \sim 160$. The low dielectric loss and high Q along the $\langle 110 \rangle$ direction are believed to relate to the different engineered domain patterns as compared to $\langle 001 \rangle$ orientation, as observed in all relaxor-PT single crystals.²⁸ The typical extensional transverse modes for perovskite ferroelectric crystal were summarized in Table I, where the first number indicates the poling direction and the second number gives the vibration orientation. Unlike $\langle 001 \rangle$ poled samples, a large discrepancy between the piezoelectric d_{31} and d_{32} was observed in $\langle 110 \rangle$ poled crystals. The optimal transverse properties were found for $(110)/\langle 001 \rangle$ cut (polarized along $\langle 110 \rangle$ with vibration along $\langle 001 \rangle$ direction), with electromechanical coupling factor k_{32} on the order of 0.91 and corresponding piezoelectric d_{32} on the order of -1420 pC/N . Higher mechanical Q values were also observed in the transverse mode for samples poled along $\langle 110 \rangle$ direction. It was found that the elastic compliances s_{ij} , which is relate to the speed of sound in the materials, exhibited strong anisotropic characteristics for both longitudinal and transverse modes, revealing that the acoustic wave propagating along the $\langle 110 \rangle$ direction was much higher than the $\langle 001 \rangle$ direction. The velocity difference is assumed to be related to the engineered domain configurations and the chemical

TABLE I. Longitudinal and transverse piezoelectric and electromechanical properties for $\langle 001 \rangle$ and $\langle 110 \rangle$ poled PIN-PMN-PT crystals.

PIN-PMN-PT	K_{ij}	Loss (%)	k_{ij}	d_{ij} (pC/N)	s_{ij}^E (pm ² /N)	Q_{ij}	
Longitudinal $ij=33$	001	4400	0.4	0.92	1500	68.0	160
	110	3400	0.2	0.91	925	34.8	500
$ij=31$	001/100	4400	0.4	0.50	-700	51.2	150
$ij=31(45^\circ)$	001/110	4400	0.4	0.81	-800	25.0	150
$ij=32$	110/001	3400	0.2	0.91	-1420	83.1	200
$ij=31$	110/-110	3400	0.2	0.74	590	21.5	210

bonds along different orientations, where a more compact crystal lattice should have higher velocity. This is under further investigation.

D. Piezoelectric properties as function of temperature

Figure 5 presents the temperature dependent characteristics of the longitudinal electromechanical coupling [Fig. 5(a)] and piezoelectric [Fig. 5(b)] properties for $\langle 001 \rangle$ and $\langle 110 \rangle$ poled PIN-PMN-PT crystals. The k_{33} for $\langle 001 \rangle$ poled crystals was found to be on the order of 0.91 at -50°C , increasing to 0.94 at 125°C , the ferroelectric phase transition temperature, above which, the k_{33} decreased to only

0.78. In contrast, the coupling for the $\langle 110 \rangle$ poled crystals was >0.90 at -50°C , slightly increased to 0.93 at a temperature of 116°C , above which, k_{33} dropped due to the $R-O$ phase transformation. The $O-T$ phase transition at 130°C was also observed in the coupling measurement. The piezoelectric coefficient d_{33} , shown in Fig. 5(b), followed a similar trend as found in the electromechanical coupling behavior, reaching its peak value at the ferroelectric phase transition temperatures.

Figure 6 gives the temperature dependent behavior of the transverse electromechanical coupling [Fig. 6(a)] and piezoelectric [Fig. 6(b)] properties for $\langle 001 \rangle$ and $\langle 110 \rangle$ poled samples along different vibration directions. It was found

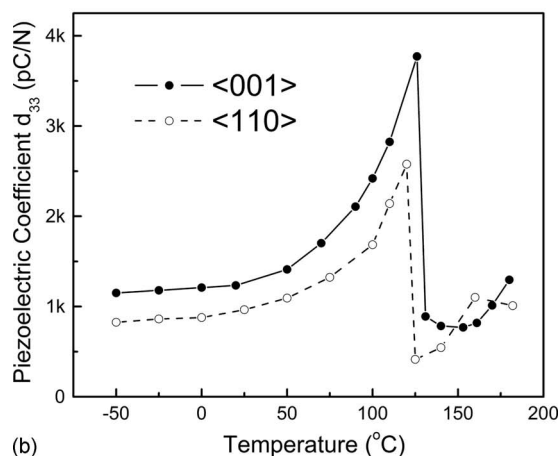
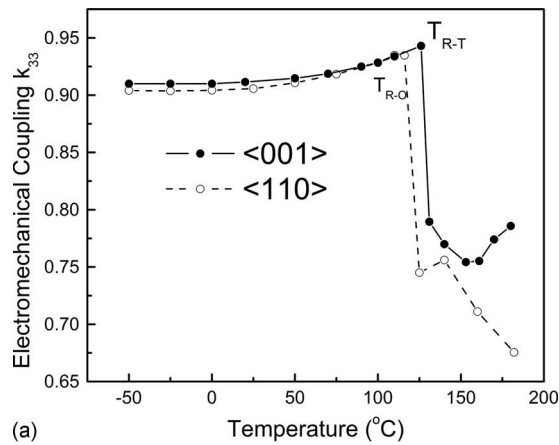


FIG. 5. Longitudinal electromechanical coupling factor k_{33} (a) and piezoelectric coefficient d_{33} (b) as a function of temperature for $\langle 001 \rangle$ and $\langle 110 \rangle$ poled single crystals.

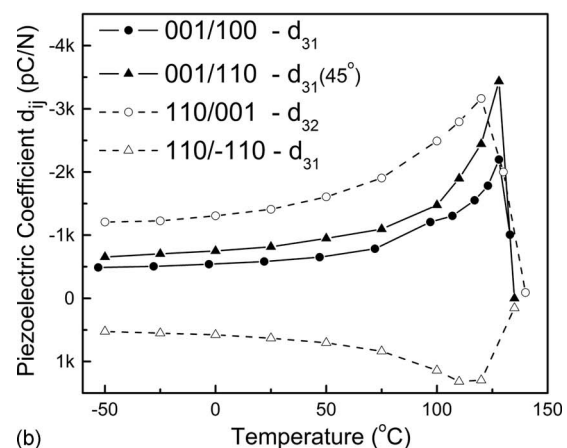
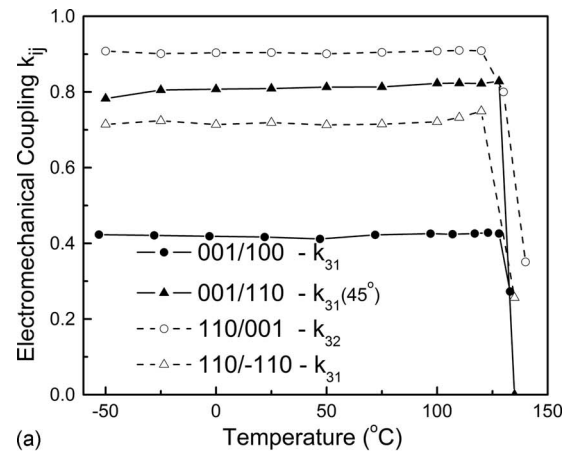


FIG. 6. Transverse electromechanical coupling factor k_{31}/k_{32} (a) and piezoelectric coefficient d_{31}/d_{32} (b) as a function of temperature for $\langle 001 \rangle$ and $\langle 110 \rangle$ poled single crystals.

that the electromechanical coupling factors k_{ij} for different poling and vibration directions followed similar tendency, maintaining their values in the temperature range from $-50\text{ }^{\circ}\text{C}$ to T_{F-F} (ferroelectric phase transition temperature). The coupling factors were found to drop sharply above the phase transition temperature, where the crystals transformed to the tetragonal and/or orthorhombic phases. The piezoelectric coefficients d_{31} and d_{32} (considering the symmetry $mm2$ in $\langle 110 \rangle$ oriented crystal, the value of d_{31} is assumed to be positive, while d_{32} is negative) showed similar temperature dependent behavior as found for the transverse coupling, reaching peak values close to the ferroelectric transition temperature, above which, the transverse piezoelectric response disappeared. From the temperature dependent properties, both $\langle 001 \rangle$ and $\langle 110 \rangle$ poled PIN-PMN-PT crystals exhibited very stable temperature dependent characteristics when compared to PMNT crystals, with a $30\text{--}40\text{ }^{\circ}\text{C}$ higher usage temperature range.

IV. CONCLUSION

In conclusion, the dielectric, piezoelectric, electromechanical, and mechanical properties were investigated as a function of orientation and temperature for PIN-PMN-PT single crystals. The longitudinal electromechanical coupling for $\langle 110 \rangle$ poled crystals showed similar value as for $\langle 001 \rangle$ orientation, while the transverse piezoelectric for $(110)/\langle 001 \rangle$ cut exhibited much higher values when compared to $\langle 001 \rangle$ poled crystals. Of particular significance is the low dielectric loss and high mechanical quality factor for $\langle 110 \rangle$ poled samples, which relates to the engineered domain configurations. Together with its broadened usage temperature range ($30\text{--}40\text{ }^{\circ}\text{C}$ higher than the binary PMNT crystal), the $\langle 001 \rangle$ and $\langle 110 \rangle$ poled PIN-PMN-PT crystals show promise for transducer and actuator applications, with the $\langle 110 \rangle$ poled crystals being an excellent candidate for high power applications where low losses are required.

ACKNOWLEDGMENTS

This work was supported by the ONR and NIH under Contract No. P41-RR11795. Thanks are due to Ms. Ru Xia for the sample preparation.

¹S. E. Park and T. R. Shrout, *J. Appl. Phys.* **82**, 1804 (1997).

²S. J. Zhang, L. Lebrun, D. Y. Jeong, C. A. Randall, Q. M. Zhang, and T. R. Shrout, *J. Appl. Phys.* **93**, 9257 (2003).

³S. J. Zhang, L. Lebrun, S. F. Liu, S. Rhee, C. A. Randall, and T. R. Shrout, *Jpn. J. Appl. Phys., Part 2* **41**, L1099 (2002).

⁴S. J. Zhang, J. Luo, R. Xia, P. W. Rehrig, C. A. Randall, and T. R. Shrout, *Solid State Commun.* **137**, 16 (2006).

⁵S. J. Zhang, C. A. Randall, and T. R. Shrout, *Jpn. J. Appl. Phys., Part 2* **42**, L1152 (2003).

⁶J. Peng, H. Luo, D. Lin, H. Xu, T. He, and W. Jin, *Appl. Phys. Lett.* **85**, 6221 (2004).

⁷R. Zhang, B. Jiang, W. H. Jiang, and W. W. Cao, *Appl. Phys. Lett.* **89**, 242908 (2006).

⁸M. Davis, D. Damjanovic, D. Hayem, and N. Setter, *J. Appl. Phys.* **98**, 014102 (2005).

⁹M. Shanthi, L. C. Lim, K. K. Rajan, and J. Jin, *Appl. Phys. Lett.* **92**, 142906 (2008).

¹⁰Y. Lu, D. Y. Jeong, Z. Y. Cheng, Q. M. Zhang, H. S. Luo, Z. W. Yin, and D. Viehland, *Appl. Phys. Lett.* **78**, 3109 (2001).

¹¹S. J. Zhang, C. A. Randall, and T. R. Shrout, *IEEE Trans. Ultrason. Ferroelectr. Freq. Control* **52**, 564 (2005).

¹²Y. H. Bing and Z. G. Ye, *J. Cryst. Growth* **250**, 118 (2003).

¹³Y. Guo, H. Luo, T. He, and Z. Yin, *Solid State Commun.* **123**, 417 (2002).

¹⁴N. Yasuda, N. Mori, H. Ohwa, Y. Hosono, Y. Yamashita, M. Iwata, M. Maeda, I. Suzuki, and Y. Ishibashi, *Jpn. J. Appl. Phys., Part 1* **41**, 7007 (2002).

¹⁵N. Yasuda, H. Ohwa, D. Hasegawa, K. Hayashi, Y. Hosono, Y. Yamashita, M. Iwata, and Y. Ishibashi, *Jpn. J. Appl. Phys., Part 1* **39**, 5586 (2000).

¹⁶Y. Hosono, Y. Yamashita, H. Sakamoto, and N. Ichinose, *Jpn. J. Appl. Phys., Part 1* **42**, 5681 (2003).

¹⁷S. J. Zhang, P. W. Rehrig, C. A. Randall, and T. R. Shrout, *J. Cryst. Growth* **234**, 415 (2002).

¹⁸S. J. Zhang, L. Lebrun, S. Rhee, C. A. Randall, and T. R. Shrout, *Appl. Phys. Lett.* **81**, 892 (2002).

¹⁹S. J. Zhang, S. Rhee, C. A. Randall, and T. R. Shrout, *Jpn. J. Appl. Phys., Part 1* **41**, 722 (2002).

²⁰S. J. Zhang, C. A. Randall, and T. R. Shrout, *Appl. Phys. Lett.* **83**, 3150 (2003).

²¹S. J. Zhang, C. A. Randall, and T. R. Shrout, *J. Appl. Phys.* **95**, 4291 (2004).

²²S. J. Zhang, S. M. Lee, D. H. Kim, H. Y. Lee, and T. R. Shrout, *Appl. Phys. Lett.* **90**, 232911 (2007).

²³A. Amin, H. Y. Lee, and B. Kelly, *Appl. Phys. Lett.* **90**, 242912 (2007).

²⁴S. J. Zhang, S. M. Lee, D. H. Kim, H. Y. Lee, and T. R. Shrout, *Appl. Phys. Lett.* **93**, 122908 (2008).

²⁵G. S. Xu, K. Chen, D. F. Yang, and J. B. Li, *Appl. Phys. Lett.* **90**, 032901 (2007).

²⁶J. Tian, P. D. Han, X. L. Huang, and H. X. Pan, *Appl. Phys. Lett.* **91**, 222903 (2007).

²⁷S. J. Zhang, J. Luo, W. Hackenberger, and T. R. Shrout, *J. Appl. Phys.* **104**, 064106 (2008).

²⁸S. J. Zhang, N. P. Sherlock, R. J. Meyer, Jr. and T. R. Shrout, *Appl. Phys. Lett.* **94**, 162906 (2009).

²⁹*IEEE Standards on Piezoelectricity* (ANSI/IEEE Standard, New York, 1987).

³⁰M. Davis, "Phase transitions, anisotropy and domain engineering: the piezoelectric properties of relaxor-ferroelectric single crystals," Ph.D. thesis, Swiss Federal Institute of Technology, 2006.

³¹D. Viehland and J. F. Li, *J. Appl. Phys.* **92**, 7690 (2002).